AD-A127 319 THRESHOLD DETECTION IN NARROWBAND NON-GAUSSIAN NOISE (U) PRINCETON UNIV NJ INFORMATION SCIENCES AND SYSTEMS LAB K S VASTOLA MAR 83 TR-9 N00014-81-K-0146 1/1

UNCLASSIFIED F/G 9/4 NL

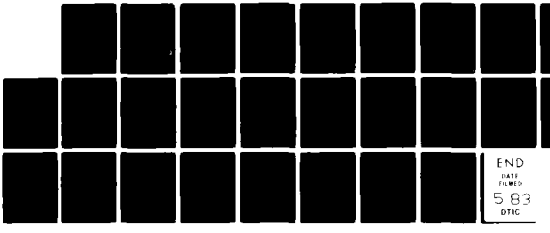

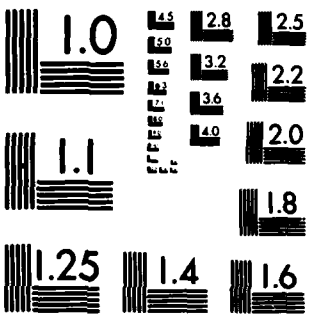

Report Number 9

THRESHOLD DETECTION IN NARROWBAND NON-GAUSSIAN NOISE

K.S. Vastola

INFORMATION SCIENCES AND SYSTEMS LABORATORY

Department of Electrical Engineering and Computer Science
Princeton University
Princeton, New Jersey 08544

MARCH 1983

Prepared for

OFFICE OF NAVAL RESEARCH (Code 411SP)
Statistics and Probability Branch
Arlington, Virginia 22217
under Contract N00014-81-K-0146
SRO(103) Program in Non-Gaussian Signal Processing

S.C. Schwartz, Principal Investigator

SECURITY CLASSIFICATION OF THIS PAGE (When Data Entered)

REPORT DOCUMENTATION PAGE		READ INSTRUCTIONS BEFORE COMPLETING FORM
1. REPORT NUMBER: 9	2. GOVT ACCESSION NO.: AD-A129 349	3. RECIPIENT'S CATALOG NUMBER
4. TITLE (and Subtitle): "Threshold Detection in Narrowband Non-Gaussian Noise"		5. TYPE OF REPORT & PERIOD COVERED: Technical Report Aug.'82-Jan.'83
		6. PERFORMING ORG. REPORT NUMBER
7. AUTHOR(s): Kenneth S. Vastola		8. CONTRACT OR GRANT NUMBER(s): N00014-81-K-0146
9. PERFORMING ORGANIZATION NAME AND ADDRESS: Information Science and Systems Lab. Dept. of Electrical Eng. & Computer Sci. Princeton University, Princeton NJ 08544		10. PROGRAM ELEMENT, PROJECT, TASK AREA & WORK UNIT NUMBERS: NR SRO-103
11. CONTROLLING OFFICE NAME AND ADDRESS: Office of Naval Research (Code 411 SP) Department of the Navy Arlington, Virginia 22217		12. REPORT DATE: March 1983
		13. NUMBER OF PAGES: 31 pages
14. MONITORING AGENCY NAME & ADDRESS(if different from Controlling Office)		15. SECURITY CLASS. (of this report): Unclassified
		15a. DECLASSIFICATION/DOWNGRADING SCHEDULE

16. DISTRIBUTION STATEMENT (of this Report)

Approved for public release; distribution unlimited

17. DISTRIBUTION STATEMENT (of the abstract entered in Block 20, if different from Report)

18. SUPPLEMENTARY NOTES

Also issued as Tech. Report. No. 46, Information Sciences and Systems Labs., EECS Dept., Princeton University.

19. KEY WORDS (Continue on reverse side if necessary and identify by block number)

Middleton Class A Model
Non-Gaussian Noise
Narrowband Noise
Locally Optimum Detection

20. ABSTRACT (Continue on reverse side if necessary and identify by block number)

The Middleton Class A narrowband non-Gaussian noise model is examined. It is shown that this noise model (which is known to fit closely a variety of non-Gaussian noises) can itself be closely approximated by a computationally much simpler noise model. It is then shown by numerical examples that, for the problem of locally optimum detection, the simplest form of this approximation yields nearly optimal (asymptotic) performance. The
(con't. on next pg.)

DD FORM 1 JAN 73 1473 EDITION OF 1 NOV 65 IS OBSOLETE
S/N 0102-LF-014-6601

SECURITY CLASSIFICATION OF THIS PAGE (When Data Entered)

(Abstract con't.)

performance of other simple suboptimal threshold detectors in Class A noise is also examined. Finally, a useful relationship between the Class A model and the ε-mixture model is developed.

Threshold Detection in Narrowband Non-Gaussian Noise

Kenneth S. Vastola
Department of Electrical Engineering and Computer Science
Princeton University
Princeton, N.J. 08544

ABSTRACT

The Middleton Class A narrowband non-Gaussian noise model [9-12] is examined. It is shown that this noise model (which is known to fit closely a variety of non-Gaussian noises) can itself be closely approximated by a computationally much simpler noise model. It is then shown by numerical examples that, for the problem of locally optimum detection, the simplest form of this approximation yields nearly optimal (asymptotic) performance. The performance of other simple suboptimal threshold detectors in Class A noise is also examined. Finally, a useful relationship between the Class A model and the ϵ-mixture model is developed.

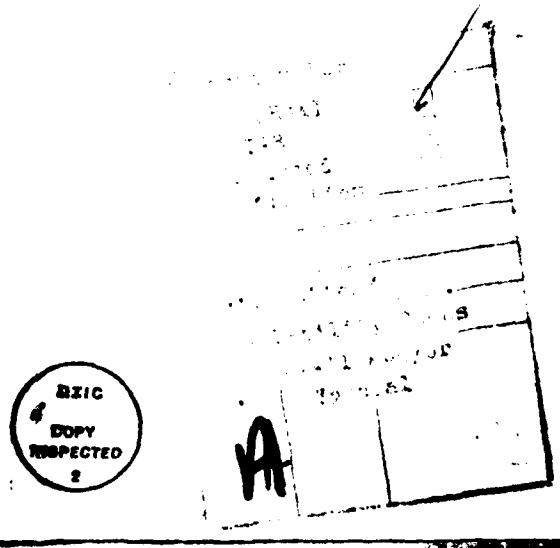

I. Introduction

For many communication problems the usual Gaussian noise assumption is inadequate. Often this is due to the occurrence of low probability, high amplitude "spikes". This impulsive component of the interference has been found to be significant in many problems. Examples include atmospheric noise, where lightning discharges in the vicinity of the receiver can cause such spikes [1-3,13-17], and underwater problems such as sonar and submarine communication, where the ambient acoustical noises may include impulses due to noisy aquatic animals such as snapping shrimp [4] or impulses due to ice cracking in arctic regions [5]. In addition to these natural non-Gaussian noise sources, there is a great variety of man-made non-Gaussian noise sources such as automobile ignitions, neon lights, and other electronic devices [6-11].

Various attempts have been made to develop models of non-Gaussian noises. These models can be divided into two groups: those which are empirically motivated and those which are physically motivated. Empirical models [13,14,18-28] are those developed to fit collected data, often with little regard for the underlying physical mechanisms. Physical models [7-12,15-17], on the other hand, attempt to model these mechanisms directly.

Among the physical models of non-Gaussian noise some of the most general are those developed by Middleton [7-12]. Middleton divides non-Gaussian noise into two classes, A and B. (There has also been consideration of a Class C which contains noises which are sums of Class A and Class B components [9].) Class B noises are broadband, i.e. those with

spectra broader than the passband of the receiver. Class A noises are narrowband, i.e. have spectra comparable to or narrower than the receiver passband.

In this paper we examine the Middleton Class A noise model. We show that, in a wide variety of cases, the first-order noise probability density function (PDF) can be closely approximated by PDF's having considerably simpler form. We then consider the locally optimum (also called threshold or weak signal) detection problem in Class A noise. We show that the detector which is locally optimum for the above PDF approximation performs very well for the original Class A model. We also examine the performance of other even simpler suboptimum threshold detectors. Finally, in Section V, a relationship is developed between the Class A noise model and the ϵ-mixture model. The ϵ-mixture model is a highly tractable empirical model, and through this relationship the advantages of the (physical) Class A model can be carried over to the mixture model, e.g., physical motivation and direct calculation of basic parameters.

II. The Class A Noise Model

Middleton [7-12] assumes the noise has the form $X(t) + N(t)$ where $N(t)$ is a Gaussian background component and

$$X(t) = \sum_j U_j(t,\vartheta) \tag{1}$$

where U_j denotes the j^{th} received waveform from an interference source and ϑ is a random parameter. He then assumes that the waveform receptions are Poisson distributed in time and shows that the normalized (to unit variance) noise density $f(x)$ can be approximated canonically by

$$f(x) = \sum_{m=0}^{\infty} K_m f(x;\sigma_m^2) \tag{2}$$

where $f(x;\sigma^2)$ is the zero-mean Gaussian PDF with variance σ^2. The variance σ_m^2 *of the* m^{th} *density is given by*

$$\sigma_m^2 = \frac{m/A + \Gamma'}{1 + \Gamma'} \tag{3}$$

and the coefficient K_m is given by

$$K_m = e^{-A}\,\frac{A^m}{m!} \tag{4}$$

where A and Γ' are the two basic parameters of the model. The first parameter, A, is called the "overlap index" and is defined by $A = \nu T$ where ν is the rate of the homogeneous Poisson process which governs the generation of the interfering waveforms U_j and T is the mean duration of a typical interfering signal. The other parameter, Γ', is given by the ratio of the power in the Gaussian portion of the interference to the power in the Poisson component. The corresponding envelope distribu-

tion is given by

$$P(E>E_0) = \sum_{m=0}^{\infty} K_m \, e^{-E_0^2/\sigma_m^2} \tag{5}$$

for $E_0 \geq 0$. Middleton has shown that, by adjusting the parameters A and Γ, the density f given in (2) can be made to fit a great variety of non-Gaussian noise densities [9-12]. Also, the parameters A and Γ are physically motivated and can be directly estimated (see [12,9]).

Unfortunately the model (2) is cumbersome. For example, in [11], Spaulding and Middleton exhibit the optimal nonlinearity for detection (i.e. the likelihood ratio $f(x-s_1)/f(x-s_0)$) and point out that this detector structure is likely to be computationally burdensome and uneconomical. Thus we would like to develop detector nonlinearities having simpler structure but which retain the desirable properties of the one given in [11].

III. Approximating the Class A Model

For each $M \geq 1$ we define the PDF f_M to be the (normalized) M-term truncation of the Class A noise PDF given in (2), i.e.

$$f_M(x) = \frac{\sum_{m=0}^{M-1} K_m f(x;\sigma_m^2)}{\sum_{m=0}^{M-1} K_m} \tag{6}$$

Since the K_m's are positive and $\sum_{m=0}^{\infty} K_m = 1$, we have that f_M (given in (6)) converges pointwise to f (given in (2)) as $M \to \infty$. (In fact, it converges uniformly.) Our goal in this section is to show that f_M is actually a very good approximation to f for small values of M. Note that f_M is a weighted sum of a finite number of Gaussian densities, a model of this form was used to model non-Gaussian noise in [22], [27] and [28].

That the Class A noise PDF given in (2) is a good model for narrowband non-Gaussian noise has been demonstrated [9-12] by showing that (for appropriate choice of parameters A and Γ) the envelope distribution (5) closely fits the measured envelope distribution of various Class-A-type noises (e.g. interference from powerlines or machinery). In Figures 1-4 we have plotted the M-term (normalized) truncation of the envelope distribution (5) for M=1,2,3,... We see that, in each case, only two or three terms are necessary in order for the truncated envelope distribution be indistinguishable from the true one. (We note that a similar observation has been made by Berry [34] concerning the instantaneous power density.) The parameters (A=0.35, Γ=0.0005) for Figure 1 are used by Middleton [9-12] to fit "interference (probably) from nearby

powerline, produced by some kind of equipment fed by line" [9]. Figure 2's parameters (A=0.0001, Γ=50) fit data from ore-crushing machinery [9-12]. The parameters of Figure 3 (A=0.1, Γ=0.001) and of Figure 4 (A=0.1, Γ=0.1) are from a range of typical values [9-12].

Figures 1-4 give rise to the hope that a detector designed to be optimal assuming the noise PDF is f_M (with M small) would perform well when the actual PDF of the noise is f. We consider here the case of "locally optimum" detection (i.e. small signal, large time-bandwidth product). The details of locally optimum detection have been presented in many places [30-33,11]. We will only state the needed results.

Under mild regularity conditions the (asymptotic) performance (or processing gain) achievable using a given detector nonlinearity $g(x)$ when the i.i.d. noise has PDF $h(x)$ is given by the efficacy functional

$$\eta(g,h) = \frac{\left[\int_{-\infty}^{\infty} g(x)h'(x)dx\right]^2}{\int_{-\infty}^{\infty} g^2(x)h(x)dx} \tag{7}$$

For a given noise PDF $h(x)$ the locally optimum detector nonlinearity $g^*(x)$ is the solution to

$$\eta^*(h) = \max_g \eta(g,h)$$

and is given by

$$g^*(x) = \frac{-h'(x)}{h(x)} \tag{8}$$

If we let $h=f_M$ in (8) we obtain the locally optimum detector nonlinearity

$g_M^*(x)$ for f_M. Since f_M is symmetric, $g_M^*(x)$ is antisymmetric (i.e. $g_M^*(-x)=-g_M^*(x)$). In Figures 5-8, $g_M^*(x)$ is plotted for the examples of Figures 1-4, respectively, for $x>0$ and M=2,3,4,... (for M=1, $g_M^*(x)$ is a straight line with slope $1/\sigma_0^2=(1+\Gamma)/\Gamma$). We see that in each case $g_2^*(x)$ closely approximates the locally optimum nonlinearity for f.

Returning to the general case, we have that for any PDF $h(x)$ the performance of its locally optimum nonlinearity $g^*(x)$ is given by

$$\eta^*(h) = \eta(g^*,h) = \int_{-\infty}^{\infty} \left[\frac{h'(x)}{h(x)}\right]^2 h(x)dx. \tag{9}$$

$\eta^*(h)$ is also known as Fisher's Information for h. An interesting (and well known) fact about the function $\eta^*(h)$ is that it is minimized by the Gaussian PDF. In fact, the locally optimum detector nonlinearity for Gaussian noise is the linear detector ($g(x)=x/\sigma^2$) which has performance equal to unity for all noise PDF's.

Since the Class A noise PDF f in (2) is highly non-Gaussian we will often have $\eta^*(f)>>1$. We have seen that for very small values of M, f_M and $g_M^*(x)$ closely approximate f and its locally optimum nonlinearity $g_f^*(x)$. So there is reason to believe that $\eta(g_M^*,f)$ should be close to $\eta^*(f)$. Table 1 bears this out. For each of the examples which we have been considering (which cover a fairly wide range of realistic values of the parameters) we see that the processing gain achievable using g_2^* is extremely close to that achievable using g_f^*.

IV. Other Simple Suboptimum Nonlinearities

In Section III we plotted locally optimum (and suboptimum) detector nonlinearities for the Class A model using logarithmic scales. In Figure 9 the locally optimum nonlinearity for the example used in Figures 1 and 5 (A=0.35, Γ=0.0005) is replotted using linear scales. The vertical dashed lines at $x = 0.06$ and $x = 0.10$ divide the x-axis into three regions $S_1 = \{|x| \leq 0.06\}$, $S_2 = \{0.06 < |x| \leq 0.10\}$, and $S_3 = \{|x| > 0.10\}$ which are the regions where $g_f^*(x)$ is approximately linear (S_1), returning to zero (S_2), and approximately zero (S_3). Evaluating the probability under f of each of these regions (or, more intuitively the fraction of the data we should expect to fall in each region) we have that $Pr(S_1) \approx 0.71$, $Pr(S_2) \approx 0.01$, and $Pr(S_3) \approx 0.28$. Thus we see that all but about 1% of the time the data will fall in the approximately linear region or the approximately zero region. This leads us to believe that g_f^* can be closely approximated by a blanker $g_{\mathcal{B}}$ (also called a hole puncher) which is shown in Figure 10a. For comparison we have also examined the performance of a soft limiter $g_{\mathcal{SL}}$ (or clipper) and a hard limiter $g_{\mathcal{HL}}$ (or sign detector) which are shown in Figures 10b and 10c, respectively.

In Table 2 we have given the processing gain achievable using the locally optimum nonlinearity g_f^*, the blanker $g_{\mathcal{B}}^*$, the soft limiter $g_{\mathcal{SL}}^*$, and the hard limiter $g_{\mathcal{HL}}$ (Note that the stars on $g_{\mathcal{B}}$ and $g_{\mathcal{SL}}$ indicate that the optimal value of c is used). We have included each of the examples given earlier as well as two others. In each case we see that the blanker is nearly optimal while the soft limiter and the hard limiter have substantially less than optimal performance. The one exception to this is the last

example (A=1.0, Γ'=0.1) where the soft limiter is nearly optimal and even the hard limiter out performs the blanker. Not surprisingly the locally optimum nonlinearity for this case (shown in Figure 11) is more closely approximated by a soft limiter than a blanker. We must stress though that, based on our experience, this seems to be an unusual case. In fact Table 2 is quite representative of our findings in general.

Another issue of importance when considering various detector nonlinearities is that of robustness or sensitivity. Since the blanker and soft limiter each only depend on one parameter (the "cut-off" parameter c), it is fairly straightforward to examine their robustness. (Note that a hard limiter does not depend on such a parameter.) In Figure 12 we plotted the processing gain achievable using $g_{\mathcal{S}}$ and $g_{\mathcal{S}_L}$ versus the cut-off parameter c for the example (A=0.35, Γ'=0.0005) considered in Figures 1, 5, and 9. It would seem from the smoothness and flatness of the curves in Figure 12 near their respective maxima that both the soft limiter and the blanker are quite insensitive to variations in the cut-off parameter.

On the other hand, in Figure 13, the same two curves are plotted using a different scale on the abscissa. This new scale is not the cut-off parameter c but the probability of the set $\{-c \le x \le c\}$ under the Class A PDF $f(x)$. As mentioned above, this can be thought of as the fraction of the data which we can expect to fall in the linear region of the detector nonlinearity (cf. S_1 in the first paragraph of this section). Since any estimate of c^*, the optimal value of the cut-off parameter, would presumably come from some version of an empirical PDF (see [12]), Figure 13 is likely to be a more reasonable way than Figure 12 to examine the sensitivity of

the blanker and soft limiter to uncertainties in estimating c^*. Results similar to Figure 13 have also been obtained for the Middleton Class B (broadband) noise model by Ingram and Houle [35].

It is not unreasonable at first thought to assume that this change in scale would cause little change in the relative smoothness and flatness of the two curves. In fact Figure 13 shows quite strikingly that the blanker is very sensitive while the soft limiter is very insensitive near their respective maxima. This example is again quite representative of a wide variety of other cases.

V. The ε-Mixture Model

In this section we consider the relationship between the ε-mixture model (defined below) and Middleton's Class A model. In the Introduction we mentioned two broad classes of models for non-Gaussian noise: physical models (such as the Middleton models) and empirical models. One commonly used empirical model is the ε-mixture (or ε-contaminated) model in which the first-order noise PDF has the form

$$f_\varepsilon(x) = (1-\varepsilon)f_0(x) + \varepsilon f_1(x) \tag{10}$$

where $\varepsilon \in [0,1]$ and f_0 and f_1 are PDF's. The PDF f_0 is usually taken to be a Gaussian PDF representing background (i.e. nonimpulsive) noise such as receiver front-end noise. Among the choices for the "contaminating" PDF f_1 are various "heavy-tailed" densities such as the Laplacian or double exponential [18,19]. Others have chosen f_1 to be also Gaussian with variance $\sigma_{f_1}^2$ taken to be many times the variance of f_0, $\sigma_{f_1}^2$. The ratio $\gamma^2 = \sigma_{f_1}^2 / \sigma_{f_0}^2$ has generally been taken to be between 1 and 100 [20-26]. As with other empirical models the disadvantage of the mixture model is that the parameters (ε and γ^2) are not directly related to the underlying physical situation and hence are difficult to determine. The primary advantage of the mixture model is its analytic simplicity.

We saw in Section III that for a wide range of values of the parameters, A and Γ', of Middleton's Class A noise model the (normalized) sum of the first two terms of the first-order noise PDF give a sufficiently accurate approximation to the full PDF given in (2). In these cases f_M is just a "Gaussian-Gaussian" mixture as in (10) with $f_0(x) = f(x;\sigma_0^2)$,

$f_1(x)=f(x;\sigma_1^2)$,

$$\gamma^2 = \frac{\sigma_1^2}{\sigma_0^2} = 1 + \frac{1}{A\Gamma'} \tag{11}$$

and

$$\varepsilon = \frac{K_1}{K_0 + K_1} = \frac{A}{1 + A} \tag{12}$$

Thus we see that, when a Gaussian-Gaussian mixture is used to model narrowband non-Gaussian noise, it may be possible to obtain ε and γ^2 from (11), (12) and the techniques already developed for determining A and Γ' [12,9].

Another interesting consequence of the relations (11) and (12) is that (at least, for Class-A-type noises) reasonable values for γ^2 seem to be between 100 and 10^4. For example, if A=0.1 and Γ'=0.001 as in Figures 3 and 7 then γ^2=10,001, and if A=0.35 and Γ'=0.0005 as in Figures 1 and 5 then γ^2=5715. These values are as much as two orders of magnitude greater than those previously used for γ^2 [20-26]. On the other hand the commonly used values of ε, say between 0.01 and 0.25, correspond approximately to values of A between 0.01 and 1/3.

VI. Summary and Conclusions

In this paper we have shown that the Middleton Class A noise model can often be approximated closely by the (normalized) sum of just the first few terms. In fact, in many cases, two terms are sufficient. This was especially clear when we looked at the efficacy of the detector nonlinearity which is locally optimum for two terms of the Class A model and found it comparable to the efficacy of the full locally optimum detector (see Table 1).

We have also examined the performance of some simple suboptimum detector nonlinearities. For most Class A noises the blanker has nearly optimal performance while the soft limiter and hard limiter have significantly lower performance. On the other hand the performance of the blanker seems to be far more sensitive to errors in estimating the optimal cut-off parameter.

Finally, for those cases where two terms of the Class A model are enough we have developed a relationship between the Class A model and the ϵ-mixture model. This yields a way of estimating the parameters of the mixture model directly from the physically motivated parameters of the Class A model.

It should also be noted that one of the clear advantages of the Middleton Class A noise model is that, since its parameters can be estimated directly from the data, any detector based on this model could easily be implemented adaptively. Such a situation would require real-time computation of the detector nonlinearity. Here the above approximation would result in substantial computational savings. Furthermore, in such

a situation it would be possible to determine M (the truncation parameter) in an adaptive fashion as well. That is, first determine A and Γ' and then choose the number of terms necessary to achieve the desired degree of approximation. In fact, this approach (of determining M adaptively) could actually be used to obtain optimal (not just nearly optimal) performance in some situations. Optimal performance could be achieved using the philosophy of the Schwartz detector (see [29] for details).

Finally we note that, while we have carried out our analysis only for the problem of locally optimum detection, the closeness of the envelope distribution approximations (Figures 5-8) encourages us to believe that similar computational savings might be realized by applying the approach of this paper to other non-Gaussian signal processing problems. Furthermore, we re-emphasize that, while our results have primarily been demonstrated by some examples, these examples cover a wide range of realistic values for the parameters of the model.

Acknowledgement

The author wishes to thank S.C. Schwartz, S.V. Czarnecki, and J.B. Thomas for helpful and stimulating discussions.

References

1. A.D. Watt and E.L. Maxwell, "Characteristics of atmospheric noise from 1 to 100 KC," *Proc. IRE*, Vol. 45, pp. 787-794, June 1957.
2. O. Ibukun, "Structural aspects of atmospheric radio noise in the tropics," *Proc. IEEE*, Vol. 54, pp. 361-367, 1966.
3. A.D. Watt, *V.L.F. Radio Engineering*. New York: Pergamon Press, 1967.
4. D.W. Lytle, "Characteristic problems of underwater communications," *IEEE Internat. Conf. Comm. Conf. Record, Vol. II*, Seattle, Washington, pp. 38-1-3, June 1973.
5. A.R. Milne and J.H. Ganton, "Ambient noise under arctic sea ice," *J. Acoust. Soc. Amer.*, Vol. 36, No. 5, pp. 855-863, May 1964.
6. E.N. Skomal, *Manmade Radio Noise*. Princeton: Van Nostrand, 1978.
7. D. Middleton, "Statistical-physical models of urban radio-noise environments, Part I: Foundations, *IEEE Trans. Electromagn. Compat.*, Vol. EMC-14, pp. 38-56, May 1972.
8. D. Middleton, "Man-made noise in urban environments and transportation systems," *IEEE Trans. Comm.*, Vol. COM-21, pp. 1232-1241, Nov. 1973.
9. D. Middleton, "Statistical-physical models of electromagnetic interference," *IEEE Trans. Electromagn. Compat*,. Vol. EMC-19, pp. 106-127, Aug. 1977.
10. D. Middleton, "Canonical non-Gaussian noise models: Their implications for measurement and for prediction of receiver performance," *IEEE Trans. Electromagn. Compat.*, Vol. EMC-21, pp. 209-220, Aug. 1979.
11. A.D. Spaulding and D. Middleton, "Optimum reception in an impulsive interference environment - Part I: Coherent detection," *IEEE Trans. Comm.*, Vol. COM-25, No. 9, pp. 910-923, September 1977.
12. D. Middleton, "Procedures for determining the parameters of the first-order canonical models of Class A and Class B electromagnetic interference," *IEEE Trans. Electromagn. Compat.*, Vol. EMC-21, pp. 190-208, Aug. 1979.
13. W.Q. Crichlow, C.J. Roubique, A.D. Spaulding, and W.M. Beery, "Determination of the amplitude-probability distribution of atmospheric radio noise from statistical moments," *J. of Research NBS*, Vol. 65D (Radio Prop.), No. 1, pp. 49-56, January 1960.
14. F. Horner and J. Harwood, "An investigation of atmospheric radio noise at very low frequencies," *Proc. Inst. Elec. Engrs.*, No. 103, Pt. B, pp. 743-751, November 1956.
15. K. Furutsu and T. Ishida, "On the theory of amplitude distribution of impulsive random noise," *J. of Applied Physics*, Vol. 32, No. 7, pp. 1206-1221, July 1961.

16. P. Beckmann, "Amplitude-probability distribution of atmospheric radio noise," *J. of Research NBS*, Vol. 68D (Radio Science), No. 6, pp. 723-736, June 1964.

17. A.A. Giordano and F. Haber, "Modeling of atmospheric noise," *Radio Science*, Vol. 7, No. 11, pp. 1101-1023, November 1972.

18. J.H. Miller and J.B. Thomas, "The detection of signals in impulsive noise modeled as a mixture process," *IEEE Trans. Comm.*, Vol. COM-24, pp. 559-563, May 1976.

19. J.W. Modestino and A.H. Levesque, "A mixture model for VLF noise with applications to M-ary spread-spectrum signaling," *Proc. Fifth Annual Princeton Conf. Inform. Sci. Sys.*, Princeton Univ., Princeton, NJ, March 25-26, 1971. (Abstract only.)

20. G.V. Trunk, "Small- and large-sample behavior of two detectors against envelope-detected sea clutter," *IEEE Trans. Inform. Theory*, Vol. IT-16, No. 1, pp. 95-99, Jan. 1970.

21 R.D. Martin and C.P.McGath, "Robust detection of stochastic signals," *IEEE Trans. Inform. Theory*, Vol. IT-20, pp. 537-541, July 1974.

22. C.J. Masreliez, "Approximate non-Gaussian filtering with linear state and observation relations," *IEEE Trans. Autom. Control*, Vol. AC- , pp. 107-110, Feb. 1975.

23. H.V. Poor, M. Mami, and J.B. Thomas, "On robust detection of discrete-time stochastic signals," *J. Franklin Inst.*, Vol. 309, No. 1, pp. 29-53, Jan. 1980.

24. J.W. Tukey, "A survey of sampling from contaminated distributions," in *Contributions to Probability and Statistics*, I. Olkin, ed., Stanford Univ. Press, Stanford, CA, pp. 448-485, 1960.

25. D.F. Andrews, P.J. Bickel, F.R. Hampel, P.J. Huber, W.H. Rogers, J.W. Tukey, *Robust Estimates of Location: Survey and Advances*, Princeton University Press, Princeton, NJ, 1972.

26. E.J. Modugno, III, *The Detection of Signals in Impulsive Noise*, Ph.D. dissertation, Dept. of EECS, Princeton University, Princeton, NJ, 1982.

27. W.S. Agee and R.H. Turner, "Robust filtering and smoothing of tracking data," *Proc. 17th Ann. Allerton Conf. Comm., Control, and Computing*, Monticello, Illinois, pp. 695-704, Oct. 1979.

28. D.L. Alspach and H.W. Sorenson, "Recursive Bayesian estimation using Gaussian sums," *Automatica*, Vol. 7, No. 4, pp. 465-479, July 1971.

29. S.C. Schwartz, "A series technique for the optimum detection of stochastic signals in noise," *IEEE Trans. Inform. Theory*, Vol. IT-15, pp. 362-369, May 1969.

30. J. Capon, "On the asymptotic efficiency of locally optimum detectors," *IRE Trans. Inform. Theory*, Vol. IT-7. pp. 67-71, April 1961.

31. D. Middleton, "Canonically optimum threshold detection," *IEEE Trans. Inform. Theory*, Vol. IT-12, No. 2, pp. 230-243.

32. E.J.G. Pitman, *Some Basic Theory for Statistical Inference*. London: Chapman and Hall, 1979.

33. C.W. Helstrom, *Statistical Theory of Signal Detection*. Oxford: Pergamon Press, 1968.

34. L.A. Berry, "Understanding Middleton's canonical formula for Class A noise," *IEEE Trans. Electromagn. Compat.* Vol. EMC-23, No. 4, pp. 337-343, November 1981.

35. R.F. Ingram and R. Houle, " Performance of the optimum and several suboptimum receivers for threshold detection of known signals in additive, white, non-Gaussian noise," *Naval Underwater Systems Center Technical Report No. 6339*. New London, Conn., November 1980.

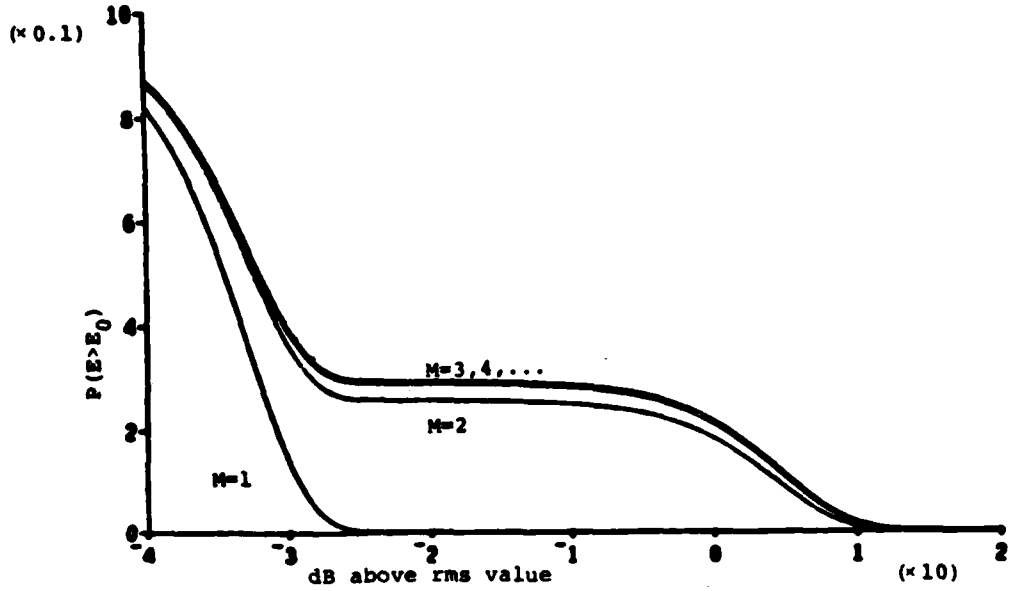

Figure 1. Truncated envelope distribution for M=1,2,3,... (A=.35,Γ=.0005).

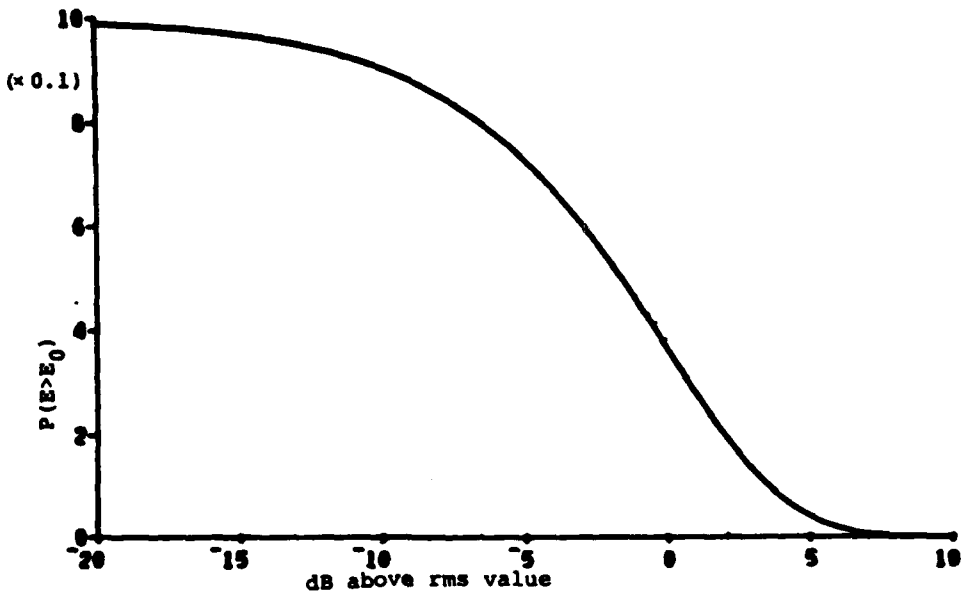

Figure 2. Truncated envelope distribution for M=1,2,3,...
(A=.0001,Γ=50).

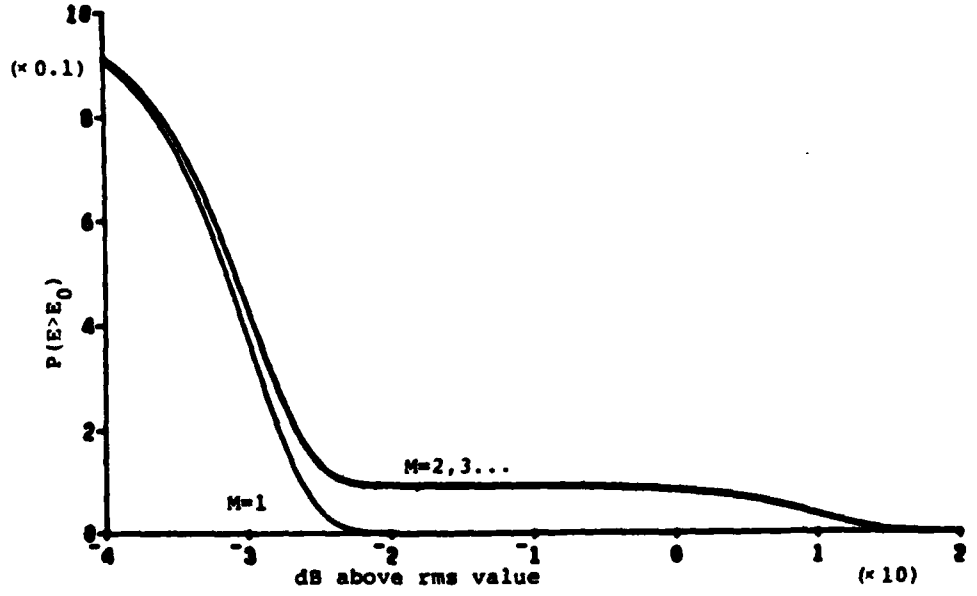

Figure 3. Truncated envelope distribution for M=1,2,3,...
(A=.1,Γ=.001).

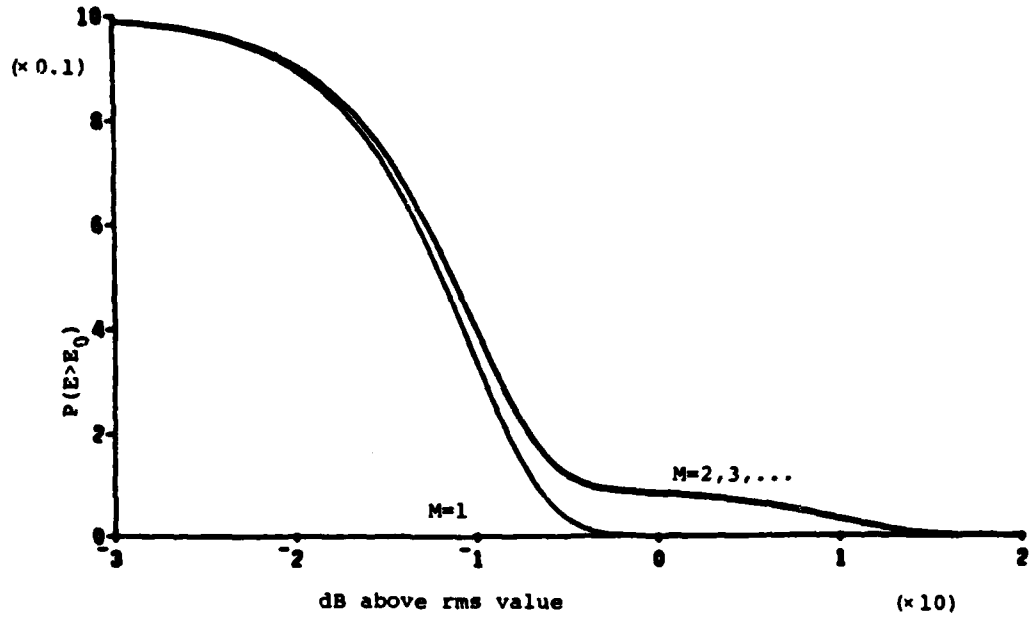

Figure 4. Truncated envelope distribution for M=1,2,3,... (A=.1,Γ=.1).

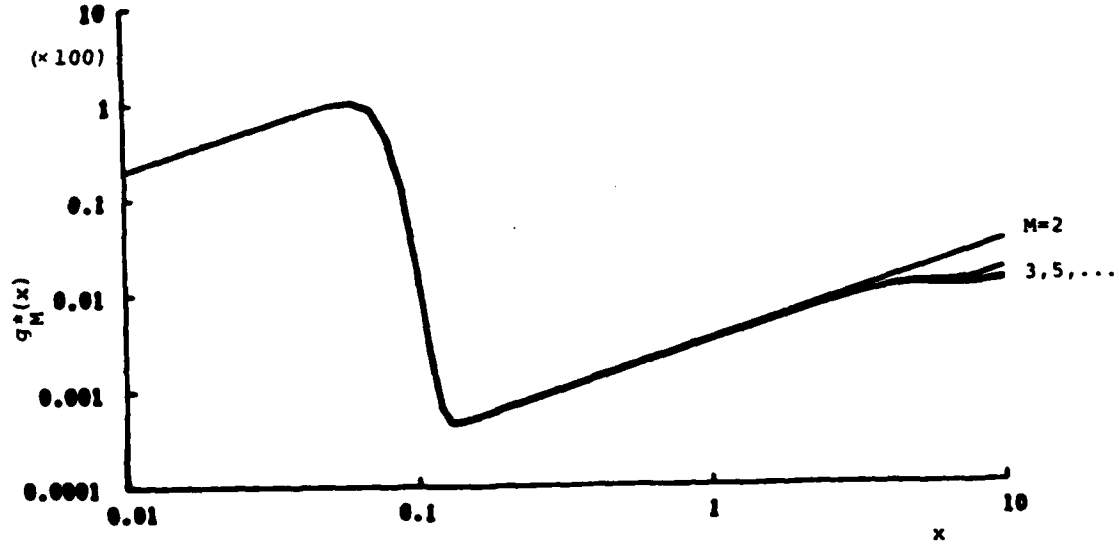

Figure 5. Locally optimum detector nonlinearity for noise PDF f_M, M=2,3,4,... (A=.35,Γ=.0005).

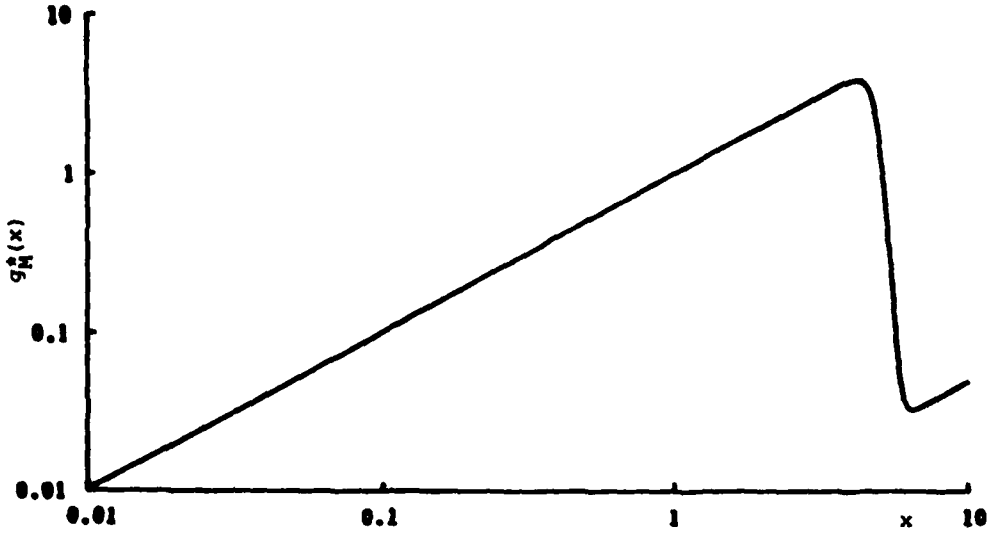

Figure 6. Locally optimum detector nonlinearity for noise PDF f_M, M=2,3,4,... (A=.0001,Γ=50).

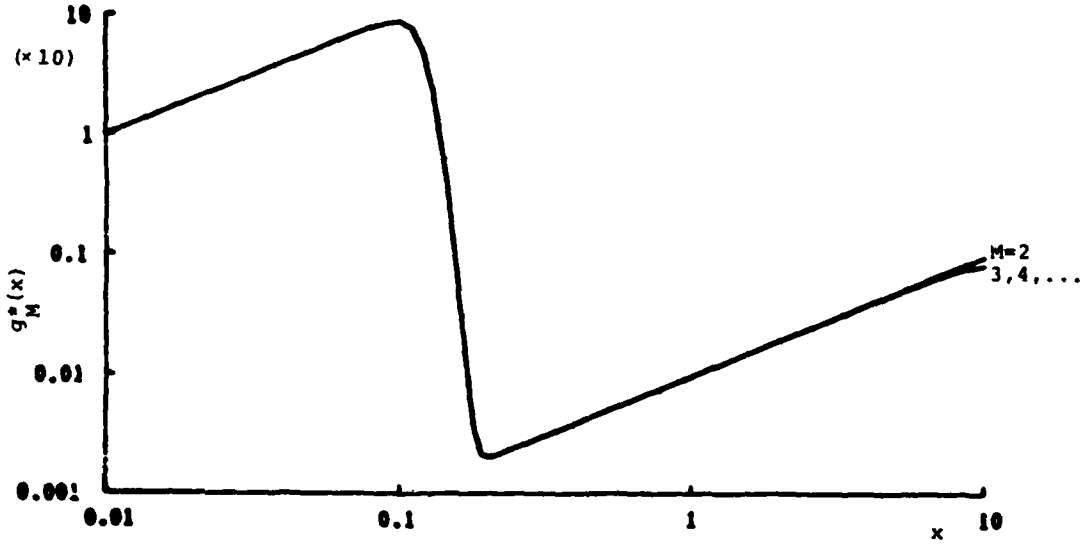

Figure 7. Locally optimum detector nonlinearity for noise PDF f_M, M=2,3,4,... (A=.1,Γ=.001).

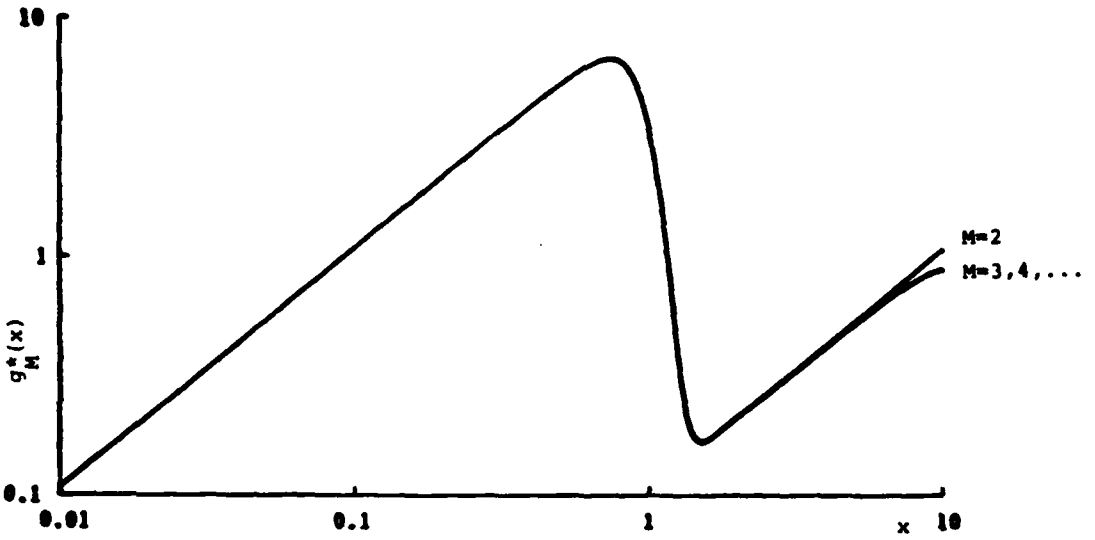

Figure 8. Locally optimum detector nonlinearity for noise PDF f_M, M=2,3,4,... (A=.1,Γ=.1).

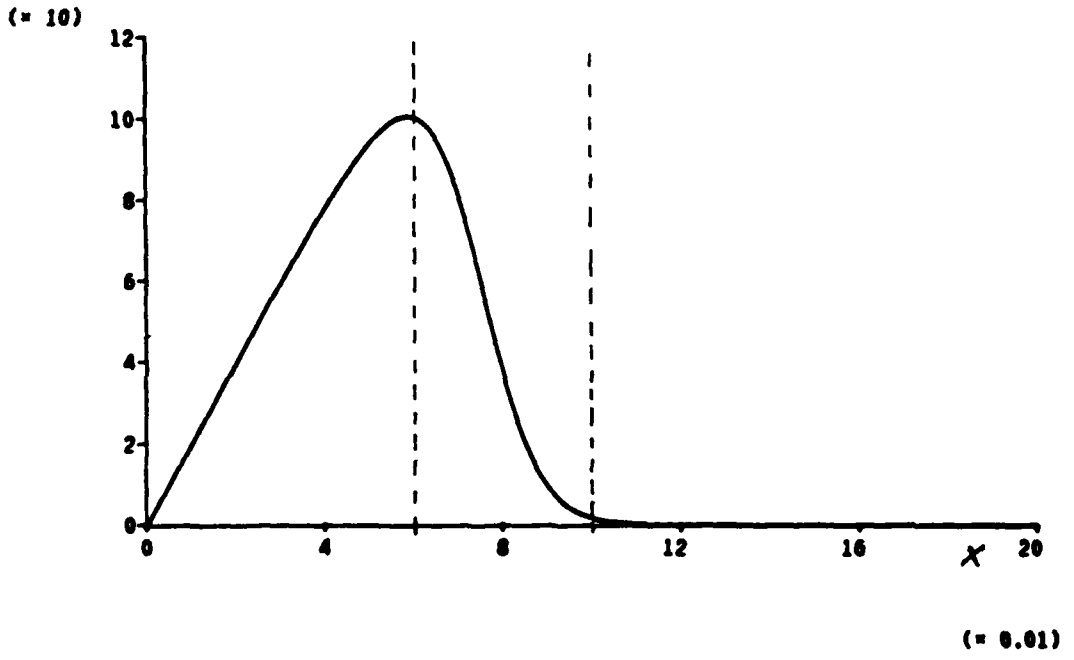

Figure 9. Locally optimum detector nonlinearity for Class A noise PDF f (linear scales) (A=0.35, Γ=0.0005).

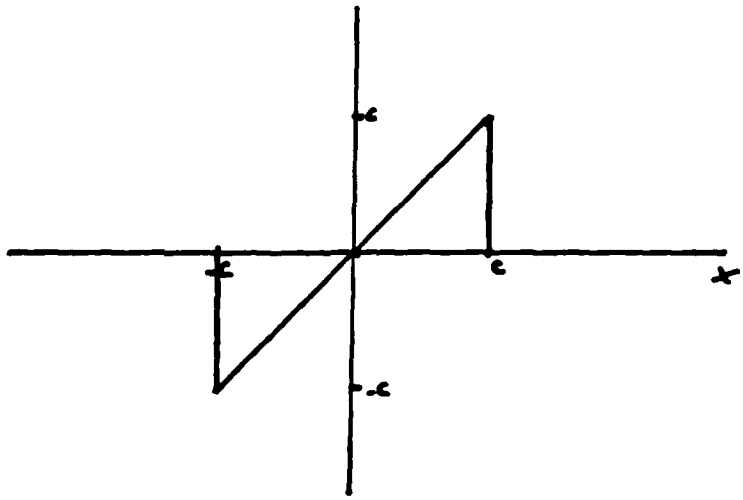

Figure 10a. The blanker (hole puncher).

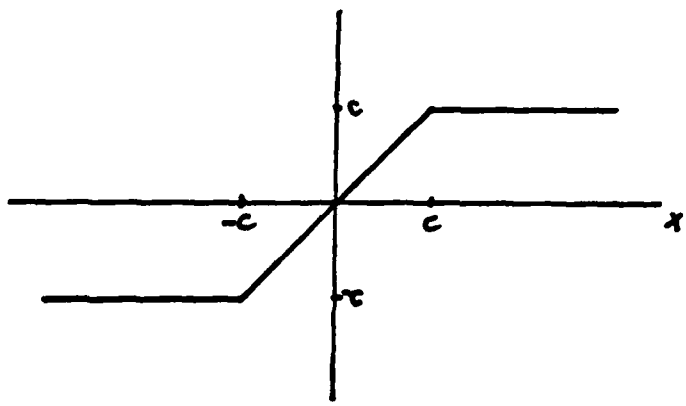

Figure 10b. The soft limiter (clipper).

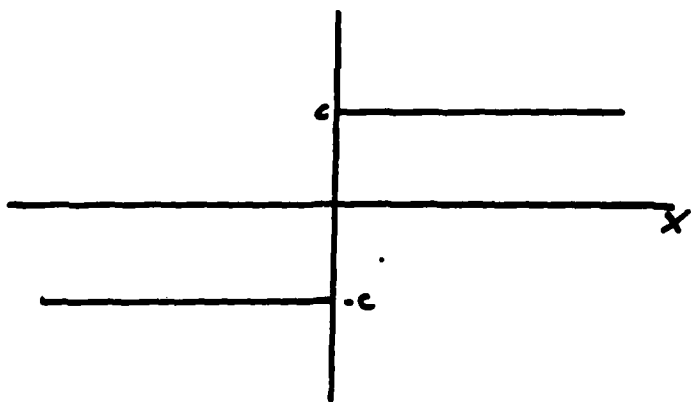

Figure 10c. The hard limiter (sign detector).

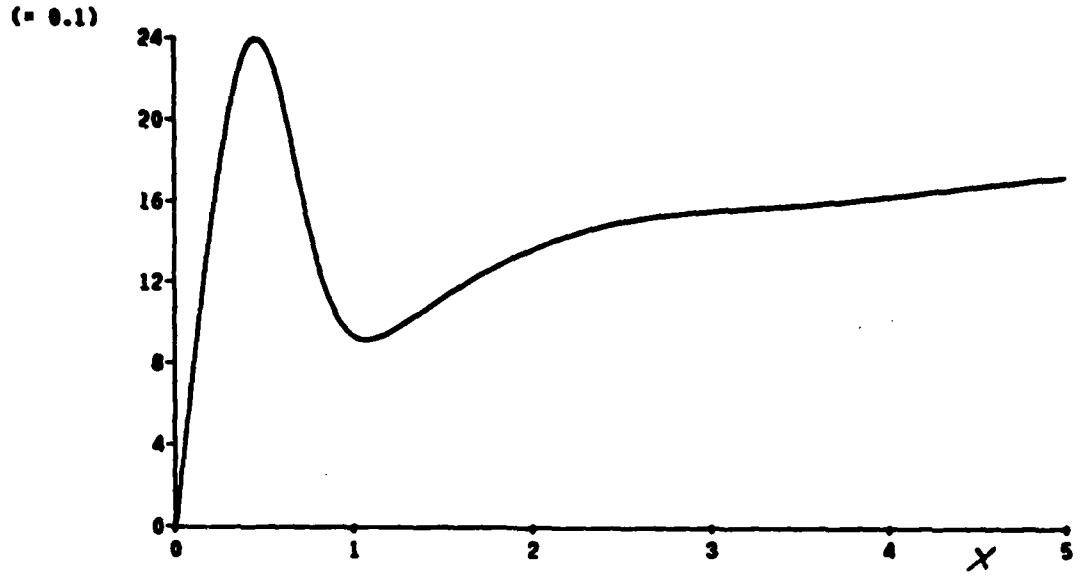

Figure 11. Locally optimum detector nonlinearity for Class A noise PDF f (linear scales) (A=1.0, Γ=0.1).

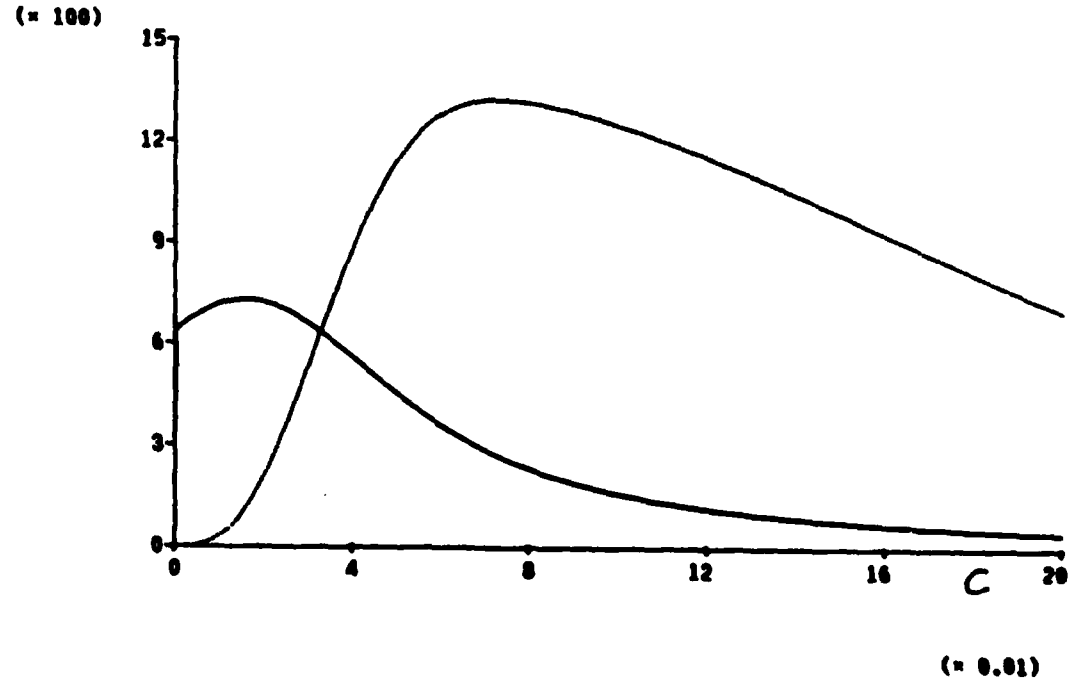

Figure 12. Efficacy (processing gain) of soft limiter $g_{SL}^{\S}$ and blanker $g_B^{\S}$ (A=0.35, Γ=0.0005).

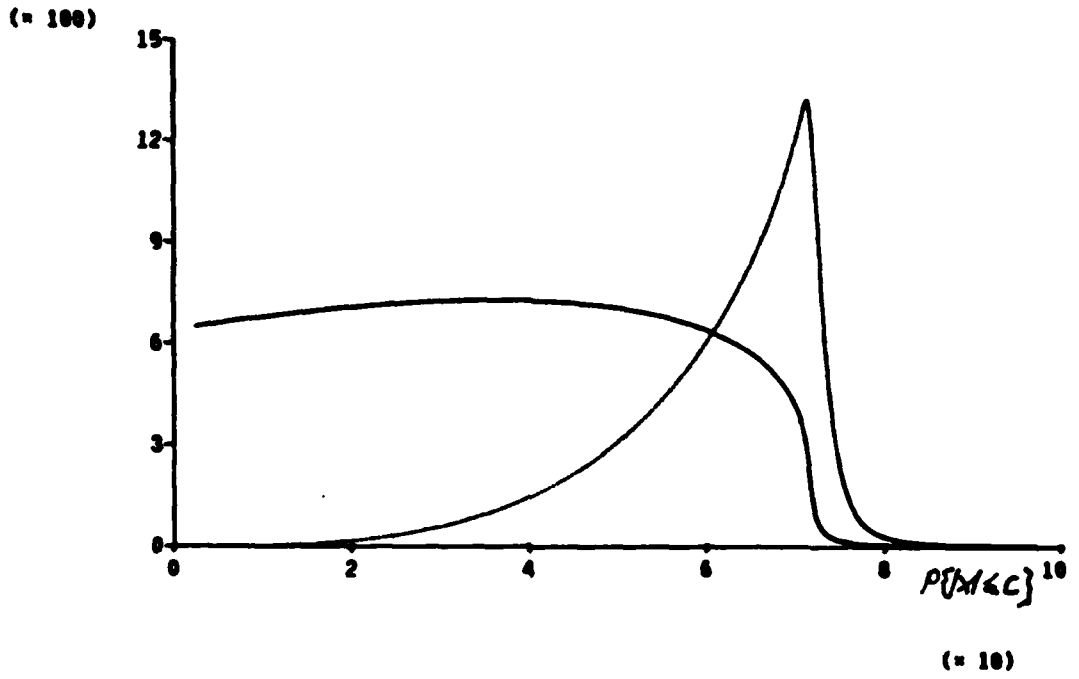

Figure 13. Efficacy (processing gain) of soft limiter g_{SL}^{ξ} and blanker g_{B}^{ξ} (A=0.35, Γ=0.0005). Abscissa scale different from Fig. 12.

M	A=0.35,Γ=0.0005	A=0.0001,Γ=50	A=0.1,Γ=0.001	A=0.1,Γ=0.1
1	1.000	1.00	1.000	1.0000
2	1339.694	1.02	892.578	9.1901
3	1340.001	1.02	892.580	9.1903
4	1340.002	1.02	892.580	9.1903

Table 1. $\eta(g_M^\bullet, f)$. Processing gain (efficacy) achievable using nonlinearity $g_M^\bullet$ in Class A noise. $\eta(g_i^\bullet, f) = L^\bullet(f)$ in all four examples.

A,Γ	0.35, 0.0005	0.0001, 50	0.1, 0.001	0.1, 0.1	1.0, 0.0001	1.0, 0.1
$g^\bullet$	1340	1.02	892.6	9.2	3299	2.39
$g^\bullet_B$	1325	1.02	890.2	9.0	3221	1.69
$g^\bullet_{SL}$	730	1.02	685.1	7.8	916	2.20
$g^\bullet_{HL}$	639	0.65	516.7	5.9	869	1.99

Table 2. Processing gain (efficacy) achievable using optimal ($g^\bullet$), blanker ($g_B^\bullet$), soft limiter ($g_{SL}^\bullet$), and hard limiter ($g_{HL}^\bullet$) nonlinearities.

OFFICE OF NAVAL RESEARCH
STATISTICS AND PROBABILITY PROGRAM

BASIC DISTRIBUTION LIST
FOR
UNCLASSIFIED TECHNICAL REPORTS

FEBRUARY 1982

	Copies
Statistics and Probability Program (Code 411(SP)) Office of Naval Research Arlington, VA 22217	3
Defense Technical Information Center Cameron Station Alexandria, VA 22314	12
Commanding Officer Office of Naval Research Eastern/Central Regional Office Attn: Director for Science Barnes Building 495 Summer Street Boston, MA 02210	1
Commanding Officer Office of Naval Research Western Regional Office Attn: Dr. Richard Lau 1030 East Green Street Pasadena, CA 91101	1
U. S. ONR Liaison Office - Far East Attn: Scientific Director APO San Francisco 96503	1
Applied Mathematics Laboratory David Taylor Naval Ship Research and Development Center Attn: Mr. G. H. Gleissner Bethesda, Maryland 20084	1
Commandant of the Marine Coprs (Code AX) Attn: Dr. A. L. Slafkosky Scientific Advisor Washington, DC 20380	1
Navy Library National Space Technology Laboratory Attn: Navy Librarian Bay St. Louis, MS 39522	1
U. S. Army Research Office P.O. Box 12211 Attn: Dr. J. Chandra Research Triangle Park, NC 27706	1
Director National Security Agency Attn: R51, Dr. Maar Fort Meade, MD 20755	1
ATAA-SL, Library U.S. Army TRADOC Systems Analysis Activity Department of the Army White Sands Missile Range, NM 88002	1
ARI Field Unit-USAREUR Attn: Library c/o ODCSPER HQ USAEREUR & 7th Army APO New York 09403	1
Library, Code 1424 Naval Postgraduate School Monterey, CA 93940	1
Technical Information Division Naval Research Laboratory Washington, DC 20375	1
OASD (I&L), Pentagon Attn: Mr. Charles S. Smith Washington, DC 20301	1

Copies

Director
AMSAA
Attn: DRXSY-MP, H. Cohen
Aberdeen Proving Ground, MD 1
21005

Dr. Gerhard Heiche
Naval Air Systems Command
(NAIR 03)
Jefferson Plaza No. 1
Arlington, VA 20360 1

Dr. Barbara Bailar
Associate Director, Statistical
Standards
Bureau of Census
Washington, DC 20233 1

Leon Slavin
Naval Sea Systems Command
(NSEA 05H)
Crystal Mall #4, Rm. 129
Washington, DC 20036 1

B. E. Clark
RR #2, Box 647-B
Graham, NC 27253 1

Naval Underwater Systems Center
Attn: Dr. Derrill J. Bordelon
Code 601
Newport, Rhode Island 02840 1

Naval Coastal Systems Center
Code 741
Attn: Mr. C. M. Bennett
Panama City, FL 32401 1

Naval Electronic Systems Command
(NELEX 612)
Attn: John Schuster
National Center No. 1
Arlington, VA 20360 1

Defense Logistics Studies
Information Exchange
Army Logistics Management Center
Attn: Mr. J. Dowling
Fort Lee, VA 23801 1

Copies

Reliability Analysis Center (RAC)
RADC/RBRAC
Attn: I. L. Krulac
Data Coordinator/
Government Programs
Griffiss AFB, New York 13441 1

Technical Library
Naval Ordnance Station
Indian Head, MD 20640 1

Library
Naval Ocean Systems Center
San Diego, CA 92152 1

Technical Library
Bureau of Naval Personnel
Department of the Navy
Washington, DC 20370 1

Mr. Dan Leonard
Code 8105
Naval Ocean Systems Center
San Diego, CA 92152 1

Dr. Alan F. Petty
Code 7930
Naval Research Laboratory
Washington, DC 20375 1

Dr. M. J. Fischer
Defense Communications Agency
Defense Communications Engineering
Center
1860 Wiehle Avenue
Reston, VA 22090 1

Mr. Jim Gates
Code 9211
Fleet Material Support Office
U. S. Navy Supply Center
Mechanicsburg, PA 17055 1

Mr. Ted Tupper
Code M-311C
Military Sealift Command
Department of the Navy
Washington, DC 20390 1

	Copies	Copies
Mr. F. R. Del Priori Code 224 Operational Test and Evaluation Force (OPTEVFOR) Norfolk, VA 23511	1	

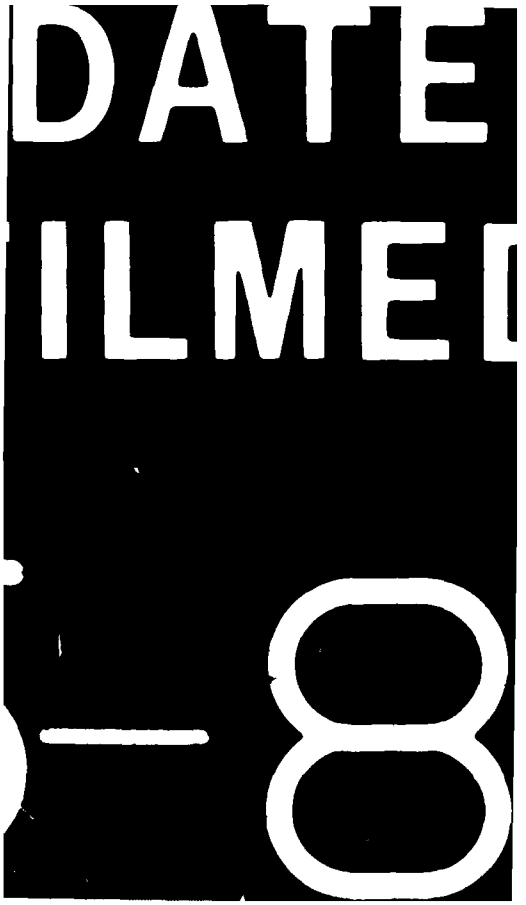
DATE
ILME
8